Proc. Natl. Acad. Sci. USA
Vol. 91, pp. 7534–7538, August 1994
Neurobiology

Linear combinations of primitives in vertebrate motor control

F. A. MUSSA-IVALDI*, S. F. GISZTER†, AND E. BIZZI

Department of Brain and Cognitive Sciences, Massachusetts Institute of Technology, Cambridge, MA 02139-4307

Contributed by E. Bizzi, April 6, 1994

ABSTRACT **Recent investigations on the spinalized frog have provided evidence suggesting that the neural circuits in the spinal cord are organized into a number of distinct functional modules. We have investigated the rule that governs the coactivation of two such modules. To this end, we have developed an experimental paradigm that involves the simultaneous stimulation of two sites in the frog's spinal cord and the quantitative comparison of the resulting mechanical response with the summation of the responses obtained from the stimulation of each site. We found that the simultaneous stimulation of two sites leads to the vector summation of the endpoint forces generated by each site separately. This linear behavior is quite remarkable and provides strong support to the view that the central nervous system may generate a wide repertoire of motor behaviors through the vectorial superposition of a few motor primitives stored within the neural circuits in the spinal cord.**

Are the neural circuits of the spinal cord organized into modules? And if these modules exist, how are they combined in order to generate complex motor behaviors? The results described here address these questions.

Recent evidence derived by focal microstimulation of the frog's spinal cord (1, 2) has revealed that the lumbar gray matter contains a number of circuits that are organized to produce muscle synergies. Whenever different circuits are activated, they produce precisely balanced contractions in different groups of muscles. The mechanical consequence of these balanced contractions is a force that may be measured at the ankle and that directs the leg toward an equilibrium point in space. Because of the changes in joint angles and in muscle lever-arms at different locations of the leg's workspace, the amplitude and direction of this force depend upon the position of the leg. Neural and biomechanical factors cooperate in the determination of a vector field that captures the dependence of the force upon the leg location.

Preliminary observations by Bizzi *et al.* (1) indicated that the simultaneous activation of two distinct spinal sites generates a field of forces proportional to the vector sum of the fields induced by the separate stimulation of each site. These preliminary observations have led to the formulation of a new framework of how the central nervous system may control motor behavior (3–5) based on the vectorial summation of a few convergent fields of the type observed in the spinalized frog. Mussa-Ivaldi and Giszter (5) found, for example, that by adding together as few as four fields converging to four different workspace locations, the central nervous system could generate not only other equilibrium positions but also fields of parallel forces as well as other more complex vectorial patterns. The descending supraspinal signals as well as local spinal reflexes may generate a variety of different fields by selecting different combinations of these modules which, in turn, would result in the vectorial superposition of the corresponding fields.

The publication costs of this article were defrayed in part by page charge payment. This article must therefore be hereby marked "*advertisement*" in accordance with 18 U.S.C. §1734 solely to indicate this fact.

The relevance of such an approach to motor control rests in part upon the assumption that the outputs of the control modules may be combined in a linear way. In this paper, we have addressed this specific issue in experimental terms. Our findings suggest that indeed, linear vector summation is a quite consistent and robust property associated with the activation of muscles and of regions of the spinal cord. This result is unexpected because of the complex nonlinearities that characterize the redundant kinematics of the limbs, the interactions among neurons, and the interactions between neurons and muscles.

METHODS

Stimulation Technique. We performed costimulation experiments on 28 spinalized bullfrogs and elicited motor responses by microstimulating the spinal cord. Our microelectrodes were placed under visual control 200–500 μm from the midline and 500–1000 μm in depth. This method of electrode placement was validated previously (2). In the costimulation experiments, the interelectrode distance range was 1 mm and 10 mm. Each stimulus consisted of a train of current impulses (300 msec). The monophasic anodal impulses had a duration of 1 msec and a frequency of 40 Hz. The peak current varied between 1 and 10 μA.

Data Recording. For each microstimulation, we collected the signals from a six-axis force transducer (ATI-310) connected to the ipsilateral ankle. The force transducer was mounted on a two-axis cartesian manipulator. We determined the location of the frog's ankle—with a resolution of 1 mm—by independently setting the x and y coordinates of this manipulator. The x–y plane corresponded approximately to the horizontal plane.

Nonredundant and Redundant Leg Kinematics. We connected the force transducer to the frog's leg in two different configurations. In the "nonredundant" configuration, the leg was attached to the transducer immediately above the ankle. In this configuration, the angles of hip and knee joints were fixed for any location of the transducer in the x–y plane.

In the "redundant" configuration, the sensor was attached to the foot by means of a low-friction gimbal arrangement, which allowed free rotation of the foot about three intersecting axes of rotation. With this redundant configuration, the joint angles of the leg could assume different values at any location of the sensor on the x–y plane.

Force Field Reconstruction. *Active and resting forces.* At each ankle location, x, and at each instant of time, t, the net force vector, $\mathbf{F}(x, t)$, obtained in response to a stimulation was expressed as the sum of two components—the "resting" force vector, $\mathbf{F}_O(x)$, and the "active" force vector, $\mathbf{F}_A(x, t)$:

$$\mathbf{F}(x, t) = \mathbf{F}_O(x) + \mathbf{F}_A(x, t).$$

*Present address: Departments of Physiology, Physical Medicine and Rehabilitation, Northwestern University Medical School, Chicago, IL 60611-3008.
†Present address: Department of Anatomy and Neurobiology, Medical College of Pennsylvania and Hahnemann University, Philadelphia, PA 19129.

The resting force field corresponded to the force measured at each location before the onset of the stimulation. By construction, this field was time-independent. If we indicate by t_O the time at which the stimulation began, we may write that:

$$\mathbf{F}_O(x) = \mathbf{F}(x, t) \; t \leq t_O.$$

The active force field, $\mathbf{F}_A(x, t)$ represented the additional force induced by our stimulation.

Measurement procedure and field interpolation. Following the same spinal or muscular stimulation, we measured the mechanical response at different locations of the ankle in the workspace (2). Typically, we recorded the force vectors in a set of nine locations arranged over a 3 × 3 grid that covered an extended region (approximately 6 × 8 cm^2) of the leg's workspace. At each grid location, we recorded the force vector elicited by the stimulation of the same spinal site or muscle.

At a single stimulation site and at a given instant of time (with respect to the onset of the stimulation), the force vectors measured at the different locations of the ankle in the workspace were considered to be samples of a continuous force field. We used the measured force vectors to estimate the force field across a broad convex region of the ankle's workspace. To this end, we implemented a piecewise, linear interpolation procedure (6). This procedure partitions the workspace into nonoverlapping triangles, as close to equilateral as possible. The vertices of each triangle were the tested grid points.

Within each triangle, the force components were given as:

$$\mathbf{F}_x = a_{1,1}x + a_{1,2}y + a_{1,3},$$

$$\mathbf{F}_y = a_{2,1}x + a_{2,2}y + a_{2,3}.$$

The six parameters, a_{ij}, were estimated by requiring that the terms $\mathbf{F}_x$ and $\mathbf{F}_y$, calculated from the above expression, be equal to the measured force components at the corner of each triangle. Hence, for each triangle, there was a particular set of interpolating parameters, $a_{i,j}$. We applied the above interpolation procedure to the force vectors collected at any given latency from the onset of the stimulus.

Equilibrium Point and Virtual Trajectory. By definition, the equilibrium point of a force field is a location at which all components of the force vanish. The presence of an equilibrium point was tested for by searching—within each interpolating triangle—for a location, (x_O, y_O), at which F_x and F_y were both zero. The temporal sequence of static equilibrium points associated with a single stimulation site is called a "virtual trajectory" (7).

The Summation Hypothesis. To test the summation hypothesis, we have developed a technique that entails comparing the field obtained from the costimulation of two sites, S_1 and S_2, with the scaled vector summation of the two fields obtained by stimulating each site independently.

We derived the scaled vector summation by means of the following procedure. First, we estimated the active fields, $\mathbf{F}_{A1}(x, t)$ and $\mathbf{F}_{A2}(x, t)$, induced by the activation of S_1 and S_2, respectively. Then, we estimated the active field, $\mathbf{F}_{AC}(x, t)$, elicited by the costimulation of S_1 and S_2, and we considered the hypothesis that

$$\mathbf{F}_{AC}(x, t) \simeq s[\mathbf{F}_{A1}(x, t) + \mathbf{F}_{A2}(x, t)], \qquad [1]$$

where $s \in R$ is a scaling coefficient to be determined by least squares (see below). The vector-summation hypothesis in its strongest form requires that $s = 1$.

The Winner-Take-All Hypothesis. We considered an alternative to the vector summation—the "winner-take-all" hypothesis—which predicts that the outcome of a costimulation overlaps with one of the evoked fields (see refs. 4 and 5.) More rigorously, the winner-take-all hypothesis is equivalent to stating:

$$\mathbf{F}_{AC}(x, t) \simeq \arg \max_{i \in \{1,2\}} [\,||\mathbf{F}_{AC}(x, t) - s\mathbf{F}_{Ai}(x, t)||^2]. \qquad [2]$$

We determined the scaling coefficient, s, and the "winner" field by minimizing the square norm of the error between the costimulation field and $s\mathbf{F}_{A1}$ and $s\mathbf{F}_{A2}$. Then we chose the solution that yielded the least error.

Analysis of Similarity. Our analysis depends upon a quantitative measure of similarity between two sampled vector fields, such as the costimulation field and the field on the right side of Eq. 1. To derive such a measure, we have defined an inner-product operation between two sampled vector fields. Let $\{\mathbf{F}_A(x_i)\}$ and $\{\mathbf{F}_B(x_i)\}$ denote two collections of force vectors sampled at N locations, $x_1, x_2, \ldots, x_N$. We define the inner product, $\langle \mathbf{F}_A, \mathbf{F}_B \rangle$, between these two sampled fields as:

$$\langle \mathbf{F}_A, \mathbf{F}_B \rangle \equiv \sum_{i=1}^{N} \mathbf{F}_A(x_i) \cdot \mathbf{F}_B(x_i), \qquad [3]$$

where "·" stands for the ordinary inner product of two cartesian vectors.

Next, we define the norm of a sampled field, $\mathbf{F}$, as:

$$||\mathbf{F}|| \equiv \langle \mathbf{F}, \mathbf{F} \rangle^{1/2} \qquad [4]$$

and the "cosine" of the angle between two sampled fields, $\mathbf{F}_A$ and $\mathbf{F}_B$, as:

$$\cos(\mathbf{F}_A, \mathbf{F}_B) \equiv \frac{\langle \mathbf{F}_A, \mathbf{F}_B \rangle}{||\mathbf{F}_A|| \cdot ||\mathbf{F}_B||}. \qquad [5]$$

Note that $-1 \leq \cos(\mathbf{F}_A, \mathbf{F}_B) \leq 1$ with the equality holding if and only if $\mathbf{F}_A$ is proportional to $\mathbf{F}_B$—that is, if and only if $\mathbf{F}_A(x_i) = c\mathbf{F}_B(x_i)$ for some $c \in R$ and for all x_i. We used this generalized cosine as a coefficient of similarity between two fields.

From the above definitions, one may readily derive the least-squares expression for s in Eq. 1:

$$s = \frac{\langle \mathbf{F}_{A\Sigma}, \mathbf{F}_{AC} \rangle}{\langle \mathbf{F}_{A\Sigma}, \mathbf{F}_{A\Sigma} \rangle},$$

where $\mathbf{F}_{A\Sigma} \equiv \mathbf{F}_{A1} + \mathbf{F}_{A2}$.

RESULTS

Summation of Muscle Fields with Nonredundant Kinematics. Our first experimental goal was to establish whether deviation from perfect similarity between sum and costimulation fields could be attributed to random fluctuations in our experimental conditions. To this end, we tested our technique in a situation where the summation property was presumed to hold exactly: the direct costimulation of two muscles in a nonredundant configuration.

Giszter *et al.* (2) and Gandolfo and Mussa-Ivaldi (8) showed that on the basis of theoretical considerations, the activation of two independent mechanical actuators in a nonredundant condition leads exactly to the vector summation of the forces generated by each actuator. In these tests, we found that the similarity between sum and costimulation fields ranged between 0.901 and 0.998. The fields corresponding to the lowest similarity value are shown in Fig. 1. We think that the experimentally observed deviation of the similarity from unity may be due to a variety of causes. These include electrodes' polarization, electrodes' motion, muscle fatigue, physiological fluctuations in the transmitter release at the

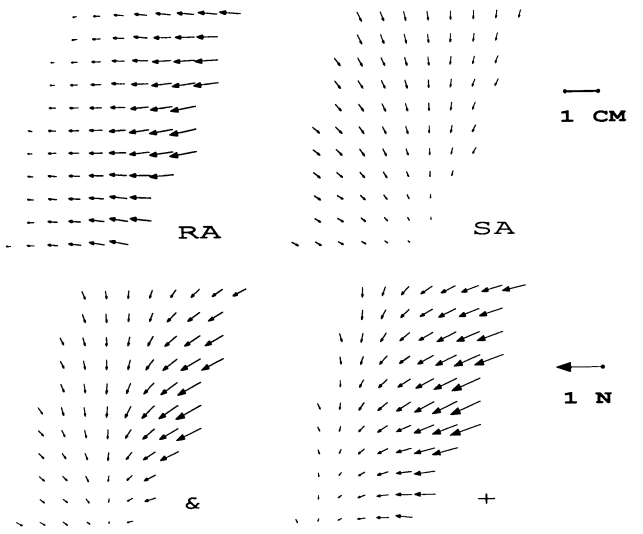

FIG. 1. Muscle costimulation with nonredundant kinematics. (*Upper Left*) Muscle field of the Rectus Anticus (RA). (*Upper Right*) Muscle field of the Sartorius (SA). (*Lower Left*) Costimulation field. (*Lower Right*) Vector summation of RA and SA. This is one of the "worst" examples of summation in the nonredundant leg. Cos = 0.901; scaling = 0.71.

neuromuscular junction, and some soft tissue motion of the leg at the point of connection with the sensor. It is reasonable to assume that some of these factors may have affected all of our microstimulation experiments. Therefore, based upon these empirical observations, we decided to use the value of 0.9 as a threshold for similarity in our subsequent analysis.

Summation of Muscle Fields with Redundant Kinematics. While vector summation of muscle forces holds exactly for a nonredundant limb, the same cannot be concluded *a priori* for a redundant serial linkage (8). The redundancy of a limb is established by the imbalance between the limb's degrees of freedom and the number of endpoint coordinates. For example, consider a leg with six rotational degrees of freedom distributed on three joints (hip, knee, and ankle). An admissible "configuration" of this leg is an array of six angles, $q = (q_1, q_2, q_3, q_4, q_5, q_6)$.

The generalized force in the configuration space of the same leg is a six-dimensional torque vector, $\tau = (\tau_1, \tau_2, \tau_3, \tau_4, \tau_5, \tau_6)$. The activation of a viscoelastic muscle, m, gives rise to a field of generalized forces in configuration space—that is, a mapping, ϕ_m, from q to τ: $\tau = \phi_m(q)$. As we are dealing with configuration space—the space of all independent degrees of freedom—and with a set of independent muscles, this mapping follows the rule of vector summation—namely, given two distinct muscles, m and n, with torque fields $\mathbf{f}_m(q)$ and $\mathbf{f}_n(q)$, the simultaneous activation of the muscles gives rise to the field:

$$\phi_c(q) = \phi_m(q) + \phi_n(q) \quad [6]$$

in generalized coordinates.

It is crucial to stress that in the above expression, we are evaluating the three fields, ϕ_c, ϕ_m, and ϕ_n at the same configuration, q. In contrast, with three different configurations, q, q', and q'', one sees that, in general,

$$\phi_\Sigma(q) \neq \phi_m(q') + \phi_n(q''). \quad [7]$$

Let us now consider the corresponding fields of endpoint forces. Each of the above muscle fields can indeed be observed by activating a muscle and measuring the endpoint force vector, $\mathbf{F} = (F_x, F_y)$, at a number of locations in the x, y plane. Let $\mathbf{F}_m(r)$, $\mathbf{F}_n(r)$ and $\mathbf{F}_c(r)$ stand for the endpoint force fields obtained by activating, respectively, muscle m, muscle n, and both of them simultaneously. Can one state that

$$\mathbf{F}_c(r) = \mathbf{F}_m(r) + \mathbf{F}_n(r)? \quad [8]$$

The answer is no. Because of the kinematic redundancy, the same location, r, in the above expression will eventually correspond to three different joint configurations, q_m, q_n, and q_c. Therefore, we are now in the case described by the inequality (Eq. 7) rather than by the Eq. 6. While the above considerations do not support vector summation in the redundant case, they are not sufficient to rule it out. To resolve this issue, we connected the force transducer at the distal end of the foot with the gimbal arrangement described in *Methods*. With this arrangement, the leg had a significant degree of mobility. In a frog of average size, when the center of the foot was held by the gimbal in the middle of the tested workspace, the joint angles at the hip, knee, and ankle could vary by about 50, 50, and 80 degrees, respectively. We performed a total of 30 muscle costimulations in seven deafferented frogs with the gimbal arrangement. We found that vector summation was adequate to describe the mechanical effects of costimulation in the vast majority of cases. The coefficient of similarity between the costimulation and the summation fields was indeed >0.9 in 83.3% of the cases (25 of 30). The average value of this similarity coefficient across the entire set of costimulations was 0.947 ± 0.04. The average value of the optimal scaling coefficient was 0.880 ± 0.213. Fig. 2 *Left* illustrates an example of vector summation. In contrast, Fig. 2 *Right* shows the outcome of one of the few muscle costimulations that did not follow vector summation. We conclude from these observations that the predominant

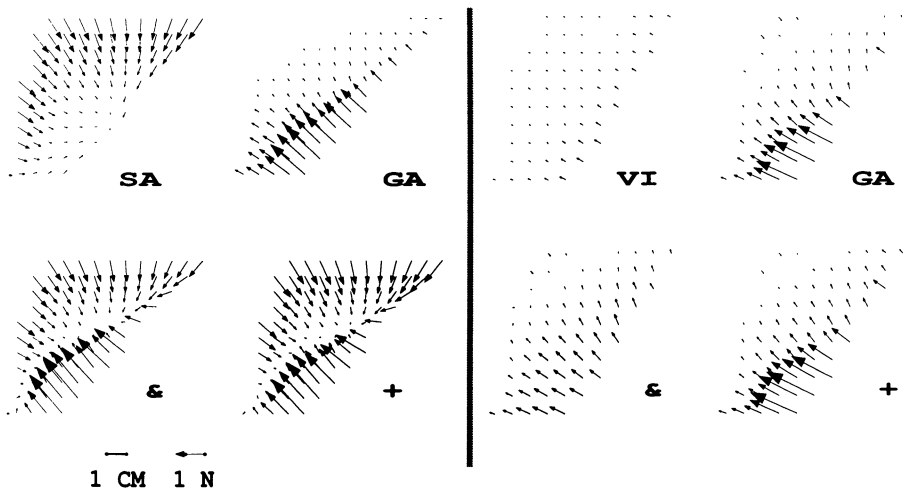

FIG. 2. Muscle costimulation with kinematic redundancy. (*Left*) Stimulation of sartorius (SA) and gastrocnemius (GA) (*Upper*); costimulation of SA and GA (&) and vector sum (+) (*Lower*). Cos = 0.986. (*Right*) Stimulation of vastus internus (VI) and gastrocnemius (GA) (*Upper*); costimulation of VI and GA (&) and vector sum (+) (*Lower*). Cos = 0.826. The data shown in *Left* and *Right* were obtained from different frogs.

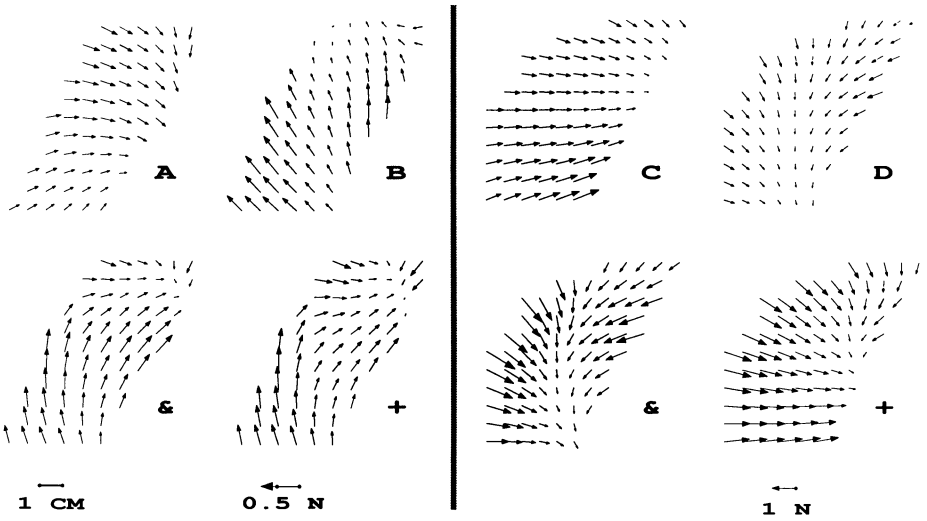

FIG. 3. Costimulation of the lumbar gray matter. (*Left*) An example of vector summation. (*Upper Left*) Fields obtained by separate stimulation of two sites, A and B. (*Lower Left*) Costimulation fields (&) and summation field (+). This was by far (87.8% of cases) the most common outcome. Cos (&/+) = 0.967. (*Right*) An example in which the costimulation (&) did not correspond to the sum (+) of the two fields (C and D) but instead to a "winner-take-all" case (D is the winner). Cos (D/&) = 0.949; Cos (+/&) = 0.770.

result of muscle coactivation was captured by the summation of the endpoint field. Surprisingly, this linear behavior was only modestly affected by the kinematic redundancy of the limb.

Summation of Fields Evoked by Microstimulation of the Spinal Cord. Once we established that the force fields of muscles add vectorially, we investigated the summation properties of the fields obtained from the microstimulation of the lumbar gray matter. As detailed in the *Methods* section, we placed two microstimulating electrodes in two distinct sites of the spinal cord. The separation between the two electrodes along the rostro-caudal direction ranged between 1 and 10 mm.

We compared the field obtained by simultaneous activation of two spinal sites against two hypotheses: the vector-summation hypothesis and the winner-take-all hypothesis. We tested each hypothesis by comparing the predicted field with the costimulation field. The hypothesis was considered to be consistent with the costimulation whenever the coefficient of similarity was >0.9. Over a total of 41 costimulation experiments, we found that the summation hypothesis was adequate to describe the costimulation field in 87.8% of the cases (36 of 41). In all of these cases, the similarity between the costimulation field and the summation field (1) was >0.9 (Fig. 3 *Left*). The average similarity across the entire data set was 0.938 ± 0.045, and the average scaling coefficient, c, was 1.077 ± 0.391, which is not significantly different from 1 at $\alpha = 0.2$ ($t = 1.230$).

We found the winner-take-all hypotheses to be consistent with the costimulation in 58.5% of cases (24 of 41). The average similarity between the winner-take-all field and the costimulation field was 0.905 ± 0.068. It is worth noting that in 53.7% of cases compatible with one or the other hypothesis, the summation and the winner-take-all hypotheses were both acceptable (i.e., they generated a similarity coefficient with the costimulation field larger than 0.9). However, in the vast majority of cases (80.5%; 33 of 41), the summation hypothesis provided a better fit for the costimulation field than the winner-take-all hypothesis. An example of a costimulation whose result was consistent with the winner-take-all hypothesis but not with the summation hypothesis is shown in Fig. 3 *Right*.

From these observations, we conclude that vector summation is clearly the prevalent combination mechanism implemented by the premotor circuitry in the frog's spinal cord.

Temporal Aspects. What are the implications of the superposition principle for the net field of forces acting upon a limb? To answer this question, we have reconstructed the total force fields, as described in the section on "Summation," from the active field and the resting field measured in a number of costimulation experiments. A typical result of this reconstruction is shown in Fig. 4. Each of the panels in this figure shows a trajectory of equilibrium points, starting from the location indicated by a filled circle. The trajectory is superimposed on the total force field corresponding to the final equilibrium point. Fig. 4 *A* and *B* represent the trajectories and the fields obtained by the separate stimulation of two spinal sites (A and B). The equilibrium trajectory and the field generated by the simultaneous stimulation of sites A and B are plotted in Fig. 4*A Lower*. Fig. 4*B Lower* shows the field and the equilibrium trajectory obtained by the vectorial summation of the fields obtained by the independent stimulation of sites A and B. The good agreement between the two lower panels provides additional support for the summation hypothesis. But maybe the most remarkable finding in this experiment is that the simple linear superposition that has been used to calculate the combined force fields has proven to be sufficient to account for the

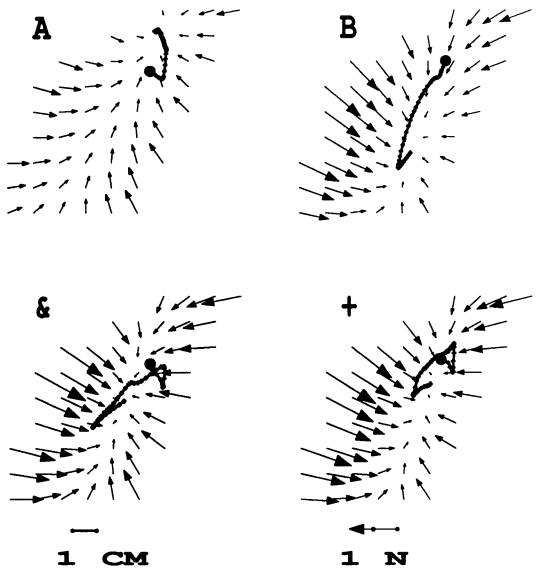

FIG. 4. Superposition of force fields and equilibrium point trajectory. The equilibrium point trajectories induced by the stimulation of two sites A and B (*Upper*) and by the costimulation (&) and the summation of the time-varying fields measured at each site (+) (*Lower*). The equilibrium point trajectories are plotted from the starting equilibrium position (indicated by the filled circle). Each trajectory is a sequence of 45 equilibrium points plotted as small crosses at 10-msec intervals. Superimposed with each trajectory is the total force field corresponding to the last equilibrium position.

complex and nonlinear "blending" of the trajectories. In the case of Fig. 4, we see that the combination leads to a loop in the endpoint equilibrium path.

DISCUSSION

The most important finding of this investigation is that the simultaneous stimulation of two premotor sites in the frog's spinal cord leads to the vector summation of the endpoint forces generated by each site separately. This finding was surprising, since we expected a number of nonlinear factors to intervene between the microstimulation and the recording of the elicited forces.

The idea that multijoint motor behavior may be organized by the central nervous system through the vectorial summation of independent elements has been pioneered by Georgopoulos *et al.* (9). These investigators suggested that individual motor cortical neurons specify a desired direction of the hand in space. According to their view, the net movement corresponding to a pattern of neural activation in the motor cortex is the vectorial sum of these individual tendencies. In our work, we have presented evidence in favor of a similar vector-summation mechanism. However, we have chosen to characterize behaviors not as positions or directions of movements, but as fields of forces over a limb's workspace.

With respect to microstimulation of the cord, the linear combination of the motor outputs generated by different spinal regions has some major functional implications for the learning and representation of motor behaviors. Most notably, linearity establishes that if a system learns to generate a set of different outputs, then the same system is also capable of generating the entire linear span of these outputs. Another intriguing consequence of linearity is that the controlling system does not need information about the internal structure of the controlled system in order to generate the entire range of possible behaviors.

A possible (and intuitive) choice for representing a reaching movement appears to be the final position of a limb or a temporal sequence of limb positions, that is a trajectory. We would like to emphasize that the vectorial summation of these vector fields is not consistent with the summation of the corresponding equilibrium postures. The vectorial summation of two fields with two different equilibrium points leads to a third field whose equilibrium is at an intermediate location. In particular, consider two linear force fields $\mathbf{F}_A(x)$ and $\mathbf{F}_B(x)$ with equilibria at x_A and x_B, respectively:

$$\mathbf{F}_A(x) = K_A(x - x_A)$$

$$\mathbf{F}_B(x) = K_B(x - x_B)$$

In this simple case, the sum field, $\mathbf{F}_\Sigma(x) = \mathbf{F}_A(x) + \mathbf{F}_B(x)$, has the equilibrium point at

$$x_\Sigma = (K_A + K_B)^{-1} \cdot (K_A\, x_A + K_B\, x_B).$$

This location is the weighted sum of x_A and x_B. Interestingly, a weighted averaging mechanism has been suggested by Lee *et al.* (10) to account for experimental observations of saccadic eye movements following the reversible deactivation of small areas in the superior colliculus. Following our approach, the weighted averaging that Lee *et al.* attribute to a more complex computational scheme can be directly obtained by assuming the vector summation of the force fields generated by the extraocular muscles.

A problematic issue arising from our investigations is that a force field is not sufficient to predict the trajectory that the limb will follow. A force field merely indicates what is the force that muscle will generate at each workspace location. The movement of the limb will result from the interactions of these forces with the inertia and the viscosity of the limb as well as the other dynamical factors. However, some of the features of an endpoint field can be directly related to motion. For example, the center of a convergent pattern of forces is an attractor point that will eventually correspond to a stable posture of the limb. In contrast, a divergent pattern of forces defines a repulsive region that the limb will tend to avoid.

This work is supported by the Office of Naval Research (N00014/88/K/0372) and the National Institutes of Health AR26710 and NS09343.

1. Bizzi, E., Mussa-Ivaldi, F. A. & Giszter, S. F. (1991) *Science* **253,** 287–291.
2. Giszter, S. F., Mussa-Ivaldi, F. A. & Bizzi, E. (1993) *J. Neurosci.* **13,** 467–491.
3. Giszter, S. (1993) *Proceedings of the Second International Conference on Simulation of Adaptive Behavior* (MIT Press, Cambridge, MA), pp. 172–181.
4. Giszter, S. (1994) *Proceedings of the Third International Conference on Simulation of Adaptive Behavior* (MIT Press, Cambridge, MA), in press.
5. Mussa-Ivaldi, F. A. & Giszter, S. F. (1992) *Biol. Cybern.* **67,** 491–500.
6. Preparata, F. P. & Shamos, M. I. (1985) *Computational Geometry* (Addison–Wesley, New York).
7. Hogan, N. (1985) *Biol. Cybern.* **52,** 315–331.
8. Gandolfo, F. & Mussa-Ivaldi, F. A. (1993) *Proc. IEEE* **3,** 1627–1634.
9. Georgopoulos, A. P., Kettner, R. E. & Schwartz, A. B. (1988) *J. Neurosci.* **8,** 2928–2937.
10. Lee, C., Rohrer, W. H. & Sparks, D. L. (1988) *Nature (London)* **332,** 357–360.